Available online at www.sciencedirect.com
SCIENCE DIRECT®
Applied Catalysis A: General 249 (2003) 365–374
APPLIED CATALYSIS A: GENERAL
www.elsevier.com/locate/apcata

A simplified partial ionic charge model to evaluate the role played by bismuth pyrostannate in multiphase catalysts for the selective oxidation of isobutene to methacrolein

L. Moens [a], P. Ruiz [b], B. Delmon [b], M. Devillers [a,*]

[a] *Unité de Chimie des Matériaux Inorganiques et Organiques, Université Catholique de Louvain, Place Louis Pasteur 1/3, B-1348 Louvain-la-Neuve, Belgium*
[b] *Unité de Catalyse et de Chimie des Matériaux Divisés, Université Catholique de Louvain, Place Croix du Sud 2/17, B-1348 Louvain-la-Neuve, Belgium*

Received 12 December 2002; received in revised form 12 March 2003; accepted 13 March 2003

Abstract

A simplified model based on partial ionic charges, developed by Jolivet to rationalise the condensation of cations in aqueous phase, is used to evaluate the electro-donating properties of binary and ternary oxide phases within the context of the remote control mechanism, in relationship with their use as heterogeneous selective oxidation catalysts. The model is applied to calculate partial ionic charges on the oxygen atoms in various binary oxides (Bi_2O_3, Sb_2O_4), or ternary systems (antimonates, phosphates, molybdates, ferrates) which are widely used in partial oxidation of alkenes. After being validated by referring to catalytic data on the partial oxidation of isobutene to methacrolein from the literature, the model is more particularly implemented to locate bismuth pyrostannate ($Bi_2Sn_2O_7$), an oxide whose interest as selective oxidation catalyst was recently demonstrated, along an already available empirical scale of donor–acceptor power of spill-over oxygen. The limitations of this simplified approach are also discussed.

Keywords: Heterogeneous catalysis; Oxides; Selective oxidation; Remote control model; Bismuth pyrostannate

1. Introduction

Most heterogeneous catalysts used in selective oxidation of alkenes are made of multiphase oxides. After many proposals aimed at proving the influence of electronic modifications of single phases, a general agreement has emerged on the fact that, in many cases, the enhanced performances result from co-operative effects between the various constituting phases. This fact is illustrated by numerous examples of highly complex industrial catalysts used nowadays in several processes. For instance, the famous multicomponent Bi-Mo-O system, which can be considered as a reference catalyst for propene oxidation to acrolein and ammoxidation to acrylonitrile (SOHIO process) was shown to be improved by incorporating simultaneously Co, Ni, Mg, Fe, Al, P and K, and, as a consequence, to contain many separate phases [1]. Another quite illustrative example is represented by the co-operation between Mo-V-W-Cu oxides and Cu, Co or Ni antimonates for the conversion of acrolein to acrylic acid [2].

* Corresponding author. Fax: +32-10-472-330.
E-mail address: devillers@chim.ucl.ac.be (M. Devillers).

0926-860X/$ – see front matter © 2003 Elsevier Science B.V. All rights reserved.
doi:10.1016/S0926-860X(03)00225-4

In all these systems, each component brings its own contribution to the global catalytic performance either through its intrinsic catalytic activity, or by modifying the physical and chemical environment (acidity, co-ordination, ...) of other elements. In the case of actual multiphase oxide catalysts, synergetic effects are invoked in the sense that the overall catalytic performances (total reactant conversion, yield and/or selectivity towards a given product) of the mixtures are enhanced with respect to the mere addition of their weighed individual contributions. The observed synergetic effects are assumed to find their origin in one of the following phenomena:

- the formation of a new catalytically active phase during the catalytic process, which is more active and/or more selective than the phases present initially in the fresh catalysts;
- the partial or total coverage of the surface of one oxide by the other oxide, resulting in the generation of a superficial contaminating phase displaying better catalytic performances;
- a "remote control mechanism" (RCM) according to which a donor phase modulates the catalytic properties of an acceptor phase, by controlling the number and nature of the active sites present at the surface of the latter. This long range interaction proceeds via migration of monoatomic oxygen species produced by the dissociative chemisorption of molecular oxygen on the surface of the donor oxide. This so-called "spill-over oxygen" moves onto the surface of the acceptor phase and, according to recent investigations at the micrometric and nanometric scale using SEM and AFM techniques on model Sb_2O_4-MoO_3 catalysts, causes surface reconstruction and/or subtle changes in surface stoichiometry. It therefore preserves a metal co-ordination state and electronic structure which make these sites highly active and selective [3–5]. Recently, Metcalfe [6,7] and Vayenas [8] independently explained the role of another sort of oxygen ion, namely that electrolytically pumped onto the surface, and the corresponding acceleration of catalytic activity. This justifies the attention paid to spill-over oxygen generation and its role in the RCM concept.

Well documented examples for which a RCM-type of mechanism has been invoked include the following cases:

- the selective oxidation of isobutene to methacrolein on mixtures between $FeSbO_4$ and Sb_2O_4 or MoO_3 [9], or on $Fe_2Mo_3O_{12}$-Sb_2O_4 mixtures [10,11],
- the partial oxidation of propane to acrolein on BiVSbO-MoO_3 or BiVSbO-Sb_2O_4 mixtures [12],
- the oxidative dehydrogenation of propane to propene on MgVO-Sb_2O_4 or $Mg_2V_2O_7$-$Mg_3V_2O_8$ [13],
- the dehydration of *N*-ethyl formamide on Sb_2O_4-MoO_3 catalysts [14],
- the dehydration and dehydrogenation of 2-butanol on SnO_2-MoO_3 or Sb_2O_4-MoO_3 catalysts [15,16], and
- the oxidative dehydrogenation of butene to butadiene using $ZnFe_2O_4$-Sb_2O_4 mixtures [10].

The RCM and the approaches of Vayenas and Metcalfe emphasise the key role of mobile oxygen species. In the frame of RCM, this justifies further investigations on the fundamental parameters involved and especially on the discovery of new potential donors of spill-over oxygen. Some years ago, Weng and Delmon tried to evaluate the donor–acceptor ability of several oxide phases in a semi-quantitative way [17]. They proposed an empirical scale of donor–acceptor power based on the magnitude of the synergetic effects observed in the yield and selectivity towards selective oxidation in the isobutene to methacrolein conversion. Their model emphasised the role of more or less polarised metal–oxygen bonds in the oxide lattice, and relied on the idea that upon adsorption of oxygen, a higher ionicity could facilitate (thermodynamic aspect) and/or accelerate (kinetic aspect) the heterolytic dissociation of oxygen at the surface, activating thereby the generation of active nucleophilic O^{2-} species, by promoting the sequence $(O_2)_g \rightarrow (O_2)_{ads} \rightarrow O_2^- \rightarrow O_2^{2-} \rightarrow O^- \rightarrow O^{2-}$.

The approach described above is directly related to the basic concepts which govern all heterogeneous oxidation reactions on oxide catalysts, and are classically known as the "Mars and van Krevelen mechanism". This mechanism includes activation of the substrate on a metal cation, insertion of surface lattice oxygen and a subsequent redox process on the catalyst surface, with replenishment of the oxygen vacancy. Moreover, according to Haber's classification of oxidation reactions, selective oxidations correspond to additions of nucleophilic oxygenated species (O^{2-}, the end species

of the above sequence) on previously activated C–H bonds. It now becomes increasingly clear that the first steps in this sequence leading to the activation of molecular oxygen are rate determining in a large number, perhaps the large majority, of catalytic processes involving oxygen (complete as well as partial oxidation). Hence, the concept underlying all reasonings, namely that both the very first step of O_2 activation and, afterwards, the degree of polarisation of the O–O bond in the intermediate species along the sequence are both important. In the RCM approach, the attention is focused on the polarisation of given chemical bonds at the surface of the donor oxide, which could induce the polarisation of O–O bond and some heterolytic splitting.

Within this context, we dedicated an extensive research program to the evaluation of bismuth pyrostannate, $Bi_2Sn_2O_7$, as selective oxidation catalyst in the isobutene to methacrolein conversion [18,19]. Careful analysis of the experimental results suggested that bismuth pyrostannate behaves as an oxygen spill-over donor with respect to WO_3 [18], and that synergetic effects between $Bi_2Sn_2O_7$ and MoO_3 (present as starting materials in the fresh catalyst) or between $Bi_2Sn_2O_7$ and α-$Bi_2Mo_3O_{12}$, a phase which is generated in situ above 400 °C during the catalytic tests, could also be considered. The migration of spill-over oxygen and the catalytic processes occurring at the surface are illustrated schematically in Fig. 1 [19]. According to this scheme, while pure $Bi_2Sn_2O_7$ does not produce any methacrolein under the selected reaction conditions, its presence in close contact with the catalytically active phases MoO_3 and α-$Bi_2Mo_3O_{12}$ results in a significant improvement of activity and selectivity in partial oxidation.

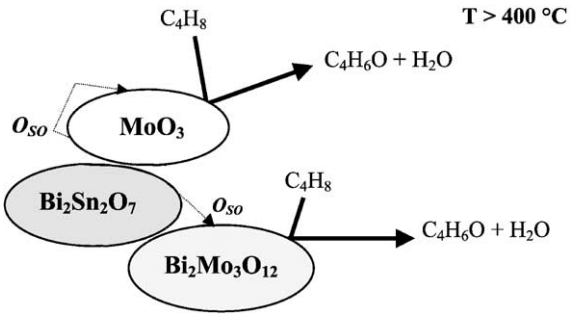

Fig. 1. Schematic view of the co-operative phenomena occurring at the surface of $Bi_2Sn_2O_7$-MoO_3 catalysts in the frame of the remote control model.

Because the catalytic data related to such phenomena accumulate in the case of some selective oxidation processes currently studied, like the oxidation of isobutene to methacrolein, it is now possible to rationalise the catalytic behaviour of these phases by referring to qualitative or semi-quantitative physico-chemical models. In a recent paper [20], we showed that fundamental concepts like ionisation energy and absolute hardness could constitute the basis of a global approach to understand the role of oxide phases as donors of spill-over oxygen within the frame of the RCM theory. In that work, we analysed the catalytic behaviour of binary lanthanide oxides Ln_xO_y in association with MoO_3, and also extended our work to ternary phases like praseodymium molybdates with various stoichiometries. In the latter case, the concepts of "average ionisation energy" and "average absolute hardness" were proposed and demonstrated to be useful tools for evaluating the ability of more complex oxide phases to give rise to co-operative effects towards selective oxidation. These "average" parameters correspond to global properties characterising the whole lattice, according to the following definition: for a ternary $(A^{m+})_x(B^{n+})_yO_z$ oxide, the "average" value P^* of the property P (ionisation energy, I, or absolute hardness, η), is calculated by $P^* = (xP(A^{m+}) + yP(B^{n+}))/(x + y)$, where the individual absolute hardnesses correspond to $(I - A)/2$, I and A representing the ionisation energy and the electron affinity of each cation, respectively.

The present paper will report on an alternative approach that consists in a generalised model defined as "partial ionic charge model" (PICM), to evaluate the donor properties of an oxide within the RCM theory. Although it refers to the same fundamental concepts, like hardness and electronegativity, this new approach emphasises an additional factor that was not considered previously, namely the influence exerted by certain structural moieties of the oxide lattice on the polarisation effects which are thought to be critically involved in the overall process of oxygen activation. Afterwards, the PICM will be applied to a case study, namely the assessment of the donor properties of bismuth pyrostannate, a ternary phase whose catalytic behaviour in the selective oxidation of isobutene to methacrolein has been investigated in detail.

2. A simplified model based on partial ionic charges

2.1. General principles

The ionic charge can be estimated using the principle of equalisation of electronegativities proposed by Sanderson [21]. This principle states that when a chemical bond forms between two atoms with different electronegativities, an electron transfer occurs till both electronegativities become equal to an average value, χ. At this point, a certain partial ionic charge is generated on each atom, defining thereby the bond polarisation. The direction of the electron transfer results from the relative values of initial electronegativities and its extent depends on the respective hardnesses of the concerned atoms, which according to Pearson's definition, measures the reluctance of a given atom to let its partial charge increase upon bonding with neighbours. This principle can be generalised to more complex moieties in which the electron transfers proceed inside a molecular entity until each atom acquires an average electronegativity value corresponding to that of the group. This value allows to calculate the partial ionic charges on each constituting atom. Our purpose is here to evaluate in that way the propensity of the donor to generate spill-over oxygen, because the ionicity within a given $[MO_x]^{z-}$ oxoanion is assumed to modulate the electro-donating power of its associated cation $(M')^{n+}$, which in turn acts on the production of the postulated spill-over oxygen species [17].

In a simplified approach proposed by Jolivet [22], the influence of neighbouring atoms has been neglected and the electronegativity is assumed to depend on the partial ionic charge only. The electronegativity of an atom i within a molecular group, χ_i, is then expressed by

$$\chi_i = \chi_i^* + \eta_i^* \delta_i \tag{1}$$

with

$$\eta_i^* = k\sqrt{\chi_i^*} \tag{2}$$

where χ_i^* is the Allred–Rochow electronegativity of the neutral atom, η^* its absolute hardness, δ the partial ionic charge, k an adjustment constant, which has been estimated originally by Sanderson on the basis on the ionic charges located on Na and F atoms in NaF, assuming 75% ionicity ($\delta(\mathrm{Na}) = -\delta(F) = 0.75$). When using the Allred–Rochow scale of electronegativity, this value is equal to 1.36. At equilibrium, Sanderson's principle of electronegativity equalisation results in $\chi_i = \chi$, and Eq. (1) becomes

$$\delta_i = \frac{(\chi - \chi_i^*)}{\eta_i^*} \tag{3}$$

Eq. (3) can be used to calculate the ionic charge on each atom within a group provided the mean electronegativity of this group is known. This value can be estimated from the chemical composition by taking into account the overall electrical charge of the group,

$$z = \sum \delta_i, \tag{4}$$

and the individual electronegativities of the constituting atoms. By combining Eqs. (2)–(4), the mean electronegativity of the anionic group $[MO_x]^{z-}$ can be calculated according to Eq. (5).

$$\chi = \frac{\sum_i \sqrt{\chi_i^*} + 1.36z}{\sum_i (1/\sqrt{\chi_i^*})} \tag{5}$$

It seems worth reminding that these partial charges are relative values in the sense that they depend on the reference used for defining the adjustment constant.

An intrinsic limitation of this simplified approach is the fact that the electronegativity values considered here are not adjusted for differences in the crystal structure. It is therefore assumed that the charge distribution is affected only by the overall chemical composition of the moiety, without any geometrical factor, as expressed by the linear relationship between χ_i and the partial ionic charge δ_i, as written above (Eq. (2)). Actually, a more rigorous treatment would introduce an additional term in Eq. (2), that takes into account the perturbation of atom i by all other atoms bound to it, located at given distances from it, and bearing their own partial charges. The present approach will therefore not allow to distinguish between the contributions of a given anionic species like $[MoO_4]^{2-}$ but in different metal molybdates displaying their own structural characteristics, even if the overall crystal structure and Mo co-ordination is the same. In summary, the structural considerations will be restricted to the ensemble of atoms which, inside a given anionic species, are considered as predominantly involved in the polarisation effects and the related electron transfer processes.

It will be shown below in the discussion on molybdates that these structural aspects can be taken into account.

2.2. Structural considerations

To estimate the magnitude of the donor character of spill-over oxygen in different oxides, we need to determine the influence of various anionic groups on the ionisation energy of a given cation. Several phases typically mentioned in works dealing with the remote control model have been considered; they contain the following oxoanions: antimonate, phosphate, ferrate, molybdate and stannate.

In some simple cases, there is no ambiguity to identify the anionic moiety which has to be taken into account. This is the case for the species $[SbO_4]^{3-}$, $[PO_4]^{3-}$ and $[Fe_2O_4]^{2-}$. In some other cases, the identification of the anionic group is not so obvious.

The particular case of the bismuth molybdate phases can be discussed by looking at their respective crystal structures [23]. In the crystal structure of α-$Bi_2Mo_3O_{12}$ (scheelite structure), stackings of $[MoO_4]^{2-}$ tetrahedra are separated by rectangular channels containing Bi^{3+} ions and cation vacancies. The $[MoO_4]^{2-}$ ion is therefore considered as the reference anionic species. In the koechlinite structure of γ-Bi_2MoO_6, alternate layers of $[BiO^+]_{2n}$ and $([MoO_6]^{2-})_n$ are present. However, the $[MoO_6]$ octahedra are highly distorted, four Mo–O bonds being much shorter than the remaining two, in such a way that the $[MoO_4]^{2-}$ moiety can also be taken as reference for that phase, even if the actual geometry of the co-ordination sphere around the Mo atom is not the same [24]. Clearly, the priority is assigned to structural fragments of the overall lattice which, due to peculiarities of the crystal structure, are assumed to be mostly responsible for the polarisation effects.

The pyrostannate phases $A_2Sn_2O_7$ display a $A_2B_2O_7$ pyrochlore-type crystal structure which is usually described as the assembly of two interpenetrating tri-dimensional lattices corresponding to $[BO_6]$ octahedra and $[A_4O]$ tetrahedra, constituting B_2O_6 and A_2O' sublattices, respectively [25,26]. In the case of bismuth pyrostannate, three polymorphs have been identified, the α-phase being the stable one from room temperature to ca. 90 °C [27]. $Bi_2Sn_2O_7$ can be viewed as the association of $[Sn_2O_6]^{4-}$ and $[Bi_2O]^{4+}$ sublattices. The first species can therefore be taken as the oxoanion and actually corresponds to the stannate ion $[SnO_3]^{2-}$, whereas $[Bi_2O]^{4+}$ can be considered as the cationic counterpart.

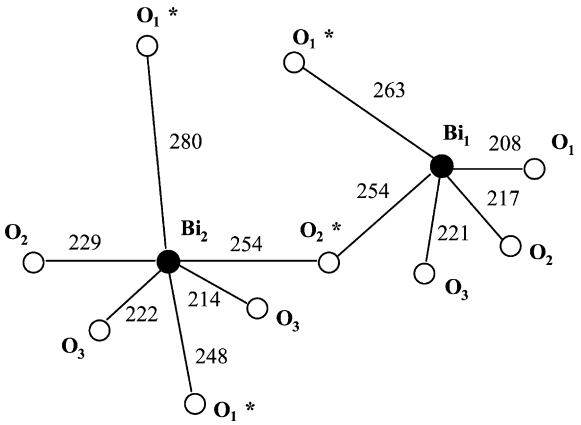

Fig. 2. Oxygen co-ordination around Bi atoms in Bi_2O_3 and atom labelling according to [28]. Bond distances given in pm.

The case of bismuth oxide itself needs to be considered in a different way. The monoclinic structure of α-Bi_2O_3, which is the stable form at room temperature, is made of alternate and equidistant layers of bismuth and oxygen atoms. When referring to the structure described by Malmros [28], illustrated in Fig. 2, two types of oxygen co-ordination appear around Bi: a six-fold octahedral co-ordination around Bi2 and a five-fold pseudo-octahedral co-ordination around Bi1. The corresponding Bi–O bond distances can be divided into two classes: the shortest ones range between 208 and 229 pm, while the longest ones lie between 248 and 280 pm and actually correspond to bridging ligands between two Bi atoms. Consequently, if four oxygen atoms out of ten are considered for one half because of their bridging nature, the virtual anionic moiety described in Fig. 2 can be identified as $[Bi_2O_8]^{10-}$, or $[BiO_4]^{5-}$. Within the frame of this model, Bi_2O_3 would be arbitrarily divided into an anionic species, $[BiO_4]^{5-}$, and a cationic species, $[Bi_3O_2]^{5+}$ ($[BiO_4]^{5-} + [Bi_3O_2]^{5+} = Bi_4O_6 = Bi_2O_3$). It is obvious that some of the anionic groups proposed are virtual species which have no real existence, but their formulation is nevertheless coherent with the crystal structure of the concerned oxides.

Table 1
Calculations of the partial oxygen charges in various oxoanions $[MO_x]^{z-}$

Oxoanion	Allred–Rochow electronegativity, $\chi^*(M^{n+})$[a]	Charge, z	Average group electronegativity, χ	Partial oxygen charge, δ_O[b]
$[BiO_4]^{5-}$	2.03	−5	0.741	−1.08
$[NbO_4]^{3-}$	1.45	−3	1.552	−0.77
$[VO_4]^{3-}$	1.56	−3	1.583	−0.75
$[SbO_4]^{3-}$	1.98	−3	1.688	−0.71
$[PO_4]^{3-}$	2.11	−3	1.718	−0.70
$[SnO_3]^{2-}$	1.89	−2	1.831	−0.66
$[Fe_2O_4]^{2-}$	1.72	−2	2.015	−0.58
$[MoO_4]^{2-}$	1.56	−2	2.045	−0.57
$[WO_4]^{2-}$	1.59	−2	2.055	−0.57

[a] χ^* oxygen = 3.5.
[b] η^* oxygen = 2.544.

2.3. Ionicity scale

The partial charges on the oxygen atoms within various oxoanions have been calculated according to the model described above and are listed in Table 1. For the species directly relevant to this work, i.e. those for which catalytic data are available in the isobutene/methacrolein conversion, the following ionicity scale could therefore be established:

$$\underset{-\delta_O=1.08}{[BiO_4]^{5-}} > \underset{-\delta_O=0.71}{[SbO_4]^{3-}} = \underset{-\delta_O=0.70}{[PO_4]^{3-}} > \underset{-\delta_O=0.66}{[SnO_3]^{2-}} > \underset{-\delta_O=0.58}{[Fe_2O_4]^{2-}} = \underset{-\delta_O=0.57}{[MoO_4]^{2-}}$$

It can therefore be concluded that, in the above series, the $[BiO_4]^{5-}$ oxoanionic moiety will lower the ionisation energy of a given cation most drastically and will be the strongest donor of spill-over oxygen.

2.4. Validation of the model

To validate the proposed model, we compared the obtained classification with the empirical scale of donor ability of oxides previously proposed by Weng and Delmon [29] (Fig. 3). This donor scale was derived from the comparison of catalytic synergies observed on methacrolein selectivity in mixtures

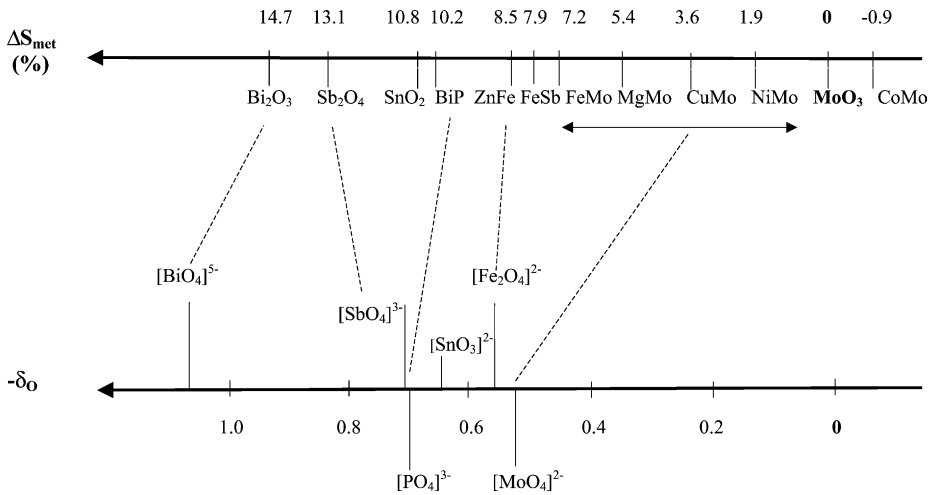

Fig. 3. Comparison between the scale of partial oxygen charges and Weng's empirical scale of donor power of spill-over oxygen [29].

between MoO_3, taken as reference acceptor phase, and different donor phases.

2.4.1. Comparison between iron(III) molybdate and iron(III) antimonate

Along the scale shown in Fig. 3, two phases contain the same cation: $Fe_2(MoO_4)_3$ and $FeSbO_4$, allowing us to examine the influence of the oxoanion on the electro-donating properties of the Fe^{3+} cation. According to the PICM proposed above, the effective charge on the oxygen of the antimonate group is larger than that in the molybdate anion. The ionicity within the antimonate moiety is therefore larger, meaning that the lowering effect on the Fe(III) ionisation energy will be larger in that case. In other words, dissociation of molecular oxygen into O^{2-} would be easier on $FeSbO_4$ than on $Fe_2(MoO_4)_3$. This is in agreement with the empirical scale proposed in Fig. 3, indicating that Fe(III) antimonate is a better donor of spill-over oxygen than Fe molybdate.

2.4.2. Comparison between Bi_2O_3 and $BiPO_4$

A similar comparison can be attempted in the case of Bi(III) oxide and phosphate, which however implies a further approximation: while Bi^{3+} can be easily identified in $BiPO_4$, our structural decomposition of Bi_2O_3 resulted in identifying virtual ionic moieties corresponding to $[BiO_4]^{5-}$ and $[Bi_3O_2]^{5+}$. Although the ionisation energies of Bi^{3+} and the virtual oxocation $[Bi_3O_2]^{5+}$ would be different, we are mainly interested in the influence of the oxoanionic group on this parameter, and not in the intrinsic values of these energies. The PICM approach predicts that the ionicity of the Bi–O bond would be higher in the $[BiO_4]^{5-}$ than in $[PO_4]^{3-}$, and consequently that Bi(III) oxide would be a more efficient donor than Bi(III) phosphate, which actually appears to be the case.

2.5. A case study: application to bismuth pyrostannate

Because the two cases described above seem to validate the PICM approach, we will now use this approach with a two-fold objective: (i) the a priori assessment of the potentialities of bismuth pyrostannate as donor of spill-over oxygen, and (ii) the location of this new donor phase along the empirical donor–acceptor scale first proposed by Weng et al.

It was already concluded from detailed investigations of the catalytic behaviour of bismuth pyrostannate in partial oxidation of isobutene that this phase would behave as a donor of spill-over oxygen. When referring to the crystal structure, the cationic species in bismuth pyrostannate would correspond to the oxocation $[Bi_2O]^{4+}$. For the same reasons as those explained earlier, we will approximate the ionisation energy of this moiety by taking the value for Bi(III), i.e. 4370 kJ/mol (45.3 eV). According to Weng's compilation [17], the best donors are characterised by ionisation energies between 3860 and 5300 kJ/mol (40–55 eV). In our recent overview of the synergetic effects on methacrolein production in mixtures of several oxides with MoO_3, we found that this optimum range remained valid in the case of more complex oxides, provided weighed, or average ionisation energies are taken into consideration when mixed valence or ternary oxides are concerned, respectively [20]. In particular, Bi^{3+} fulfils the requirement mentioned above and could consequently give rise to suitable donors of spill-over oxygen when associated with a adequate oxoanion. According to the PICM model, the partial charge on the oxygen atoms of the stannate ion is −0.66, a value which is close to that of the antimonate, and somewhat larger than that of the molybdate ion, thereby revealing a significant ionicity level. This conclusion agrees perfectly well with the experimental observation that the synergetic effects towards methacrolein production are more pronounced when MoO_3 is mixed with $Bi_2Sn_2O_7$ than with $Bi_2Mo_3O_{12}$ [18].

The PICM approach can also be used to locate this new donor phase along the donor–acceptor scale proposed by Weng. In particular, the question arises as to whether bismuth pyrostannate is a more efficient donor than Sb_2O_4 or Bi_2O_3, a question which cannot be answered directly by the experiment because the mixtures between $Bi_2Sn_2O_7$ and these two phases were found to produce no methacrolein at all [18].

The comparison between $Bi_2Sn_2O_7$ and Bi_2O_3 is straightforward provided the cationic species present in the two lattices are considered as similar. Because the ionicity within the $[BiO_4]^{5-}$ anion is larger than for $[SnO_3]^{2-}$, the first one will decrease the ionisation energy of Bi(III) more than the second one, leaving Bi_2O_3 as a stronger donor than $Bi_2Sn_2O_7$.

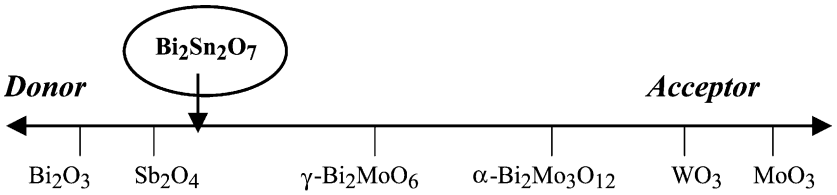

Fig. 4. Localisation of $Bi_2Sn_2O_7$ along Weng's donor–acceptor scale of spill-over oxygen.

The comparison between $Bi_2Sn_2O_7$ and Sb_2O_4 requires to take two parameters into account: the ionisation energy of the two cations involved and the ionicity within the anionic group. In this approach, Sb_2O_4 can be virtually divided into Sb^{3+} and $[SbO_4]^{3-}$. While the ionisation of Bi(III) is 4370 kJ/mol (45.3 eV), that of Sb(III) amounts to 4260 kJ/mol (44.2 eV). These values are similar and it can be assumed that, when associated to a given oxoanion, they will result in oxygen spill-over donors of similar strengths. Considering that the partial charges on the oxygen atoms are slightly higher in the antimonate anion (−0.71 instead of −0.66), the combination of these two factors suggests that Sb_2O_4 would be a slightly stronger donor than $Bi_2Sn_2O_7$, as illustrated in Fig. 4. The fact that the three oxides are close neighbours on that scale explains why their mixtures do not produce methacrolein: none of them can efficiently play the role of acceptor, namely the phase where the catalytic reaction occurs and where catalytic sites are created by spill-over oxygen. This explanation is the same as that of the lack of activity of Sb_2O_4, in spite of the fact that it contains two types of Sb ions (Sb^{3+} and Sb^{5+}).

The catalytic behaviour of bismuth pyrostannate when mixed with an acceptor phase can also be analysed in the light of some previously reported considerations. In a previous paper, already mentioned, dealing with the rationalisation of catalytic data concerning the use of mixtures of various phases with MoO_3 in the isobutene to methacrolein conversion, it was shown that the concepts of "average ionisation energy" and "average absolute hardness" were helpful to understand the magnitude of the synergetic effects on selective oxidation [20]. When comparing different oxygen spill-over donor phases, an overview of numerous literature data concluded that the catalytic behaviour was actually representative of well-adjusted electro-donating properties, and that ionisation energy values in the range 50–60 eV were particularly appropriate. This results in "volcano-type" plots of synergetic effects on methacrolein selectivity versus ionisation energy, as described in [20]. Weak ionisation energies result in the easy generation of a series of electrophilic oxygen species leading to total oxidation, while ionisation energies beyond a certain limit will decrease the rate of electron transfer in such an extent that the overall activity becomes insufficient. As indicated in Table 2, the large synergetic effects observed in the $Bi_2Sn_2O_7$-MoO_3 mixtures, compared to the $Bi_2Sn_2O_7$-$Bi_2Mo_3O_{12}$ mixtures, are once again

Table 2
Catalytic performances of mixtures with MoO_3 (50 wt.% MoO_3) in isobutene oxidation

	T[a] (°C)	I^*[b] (eV)	η^*[c] (eV)	ΔX^*[d] (%)	ΔY^*_{met}[e] (%)	ΔS^*_{met}[f] (%)
$Bi_2Sn_2O_7$-MoO_3	375	58.8	12.8	86	140	16
	400			116	480	117
$Bi_2Mo_3O_{12}$-MoO_3	375	94.2	21.4	−8	−2	7
	400			31	73	33

[a] Reaction temperature (for experimental details, see [18]).
[b] Average ionisation energy as defined in [20].
[c] Average absolute hardness as defined in [20].
[d] Synergetic effect on isobutene conversion, as defined in [20].
[e] Synergetic effect on the yield in methacrolein, as defined in [20].
[f] Synergetic effect on methacrolein selectivity, as defined in [20].

in line with an average ionisation of 58.8 eV, i.e. a value fitting perfectly well the optimal range mentioned above, while α-$Bi_2Mo_3O_{12}$ is characterised by a quite higher value (94.2 eV).

2.6. Limitations of the PICM model

As already mentioned, the most obvious limitation comes, in principle, from the fact that the calculations presented above do not take into account the structural parameters which could influence the partial ionic charge on the various atoms of a same ionic moiety. It should however be realised that, in practice, these structural aspects are of limited use in dispersed catalysts: first, because several crystal faces can contribute to the reaction, and also because surface rearrangements modify the shape and orientation of the metal–oxygen bonds involved [3].

A second limitation of the present approach is related to the way it considers the influence of the cationic counter-ion associated with the oxoanion. As explained above, the calculations of partial charges are performed on the basis of structural moieties which, inside each crystal structure, have been identified for their relevance to the polarisation effects in the lattice. This leads to the fictitious separation of the oxide lattice into a representative anionic moiety and a cationic counterpart. This cation is sometimes an imaginary species although being a realistic piece of the solid state structure. To illustrate this statement and justify the choice of the anionic moiety considered as being representative of the polarisation effects, let us go back to the comparison between α- and γ-Bi molybdates. Although the stoichiometry of the oxoanion is "chemically" different, structural considerations described above (Section 2.2) suggested to refer in both cases to the $[MoO_4]^{2-}$ species. The alternative way would have been to consider the $[MoO_6]^{6-}$ moiety. The calculation of the partial ionic charge on oxygen atoms would then provide a value of −1.08, i.e. close to that of $[BiO_4]^{5-}$. When looking at Weng's scale displayed in Fig. 4, this charge would overestimate the donor character of Bi_2MoO_6 by putting it beyond that of Sb_2O_4, in contradiction with the experimental data. This justifies our approach.

A third comment on this approach should be added: the number of anionic species directly interacting with a given reference cation can reasonably be assumed to play a role by modifying the ionisation energy of the cation, as stated above. However, simple simulations based on the overall stoichiometry of the oxide phase showed that they were not successful in accounting for their respective catalytic behaviours.

Finally, it should be remembered that heterogeneous catalysis is a phenomenon involving essentially, although not exclusively, the surface of the solid, and that the calculations described above consider that the surface and bulk compositions of the catalysts are the same.

3. Conclusions

These considerations show that a simplified partial charge model constitutes a useful tool for an a priori evaluation of the spill-over oxygen donor character of new phases. More particularly, it allows one to predict the behaviour of a given oxide when mixed with another one acting as acceptor of spill-over oxygen, in order to adapt their catalytic properties to each other. This approach seems to be quite complementary to that based on the concepts of average ionisation energy and average absolute hardness, previously described and used in the case of ternary oxide phases. Although the proposed approach is semi-empirical and the resulting scale not strictly quantitative, it has the merit of showing how the use of well-established fundamental properties can help to evaluate the complex behaviour of oxidation catalysts.

Acknowledgements

The financial support from the Belgian National Fund for Scientific Research (FNRS), Brussels, is greatly acknowledged.

References

[1] R.K. Grasselli, G.H. Heights, H.F. Hardman, US Patent 3,642,930 (1972).
[2] S. Breiter, M. Estenfelder, H.G. Lintz, A. Tenten, H. Hibst, Appl. Catal. A: Gen. 134 (1996) 81.
[3] E.M. Gaigneaux, P. Ruiz, B. Delmon, Catal. Today 32 (1996) 37.
[4] E.M. Gaigneaux, P. Ruiz, E.E. Wolf, B. Delmon, Appl. Surf. Sci. 121–122 (1997) 552.

[5] E.M. Gaigneaux, H.M. Abdel Dayem, E. Godard, P. Ruiz, Appl. Catal. A: Gen. 202 (2000) 265.
[6] I.S. Metcalfe, J. Catal. 199 (2001) 247, and 259.
[7] I.S. Metcalfe, Stud. Surf. Sci. Catal. 138 (2001) 181.
[8] C. Vayenas, S. Brosda, Stud. Surf. Sci. Catal. 138 (2001) 197.
[9] S.R.G. Carrazan, L. Cadus, Ph. Dieu, P. Ruiz, B. Delmon, Catal. Today 32 (1996) 311.
[10] L.T. Weng, Y.L. Xiong, P. Ruiz, B. Delmon, in: S. Yoshida, N. Takesawa, T. Ono (Eds.), Catalytic Science and Technology, vol. 1, Kodansha/VCH, Tokyo/Weinheim, 1991, p. 207.
[11] L.T. Weng, L. Cadus, P. Ruiz, B. Delmon, Catal. Today 11 (1992) 455.
[12] E.M. Gaigneaux, F. Englebert, P. Ruiz, Stud. Surf. Sci. Catal. 138 (2001) 145.
[13] S.R.G. Carrazan, C. Peres, J.P. Bernard, M. Ruwet, P. Ruiz, B. Delmon, J. Catal. 158 (1996) 452.
[14] B. Zhou, E. Sham, T. Machej, P. Bertrand, P. Ruiz, B. Delmon, J. Catal. 132 (1991) 157.
[15] E.M. Gaigneaux, D. Herla, P. Tsiakaras, U. Roland, P. Ruiz, B. Delmon, Am. Chem. Soc. Symp. Ser. 638 (1996) 330.
[16] E.M. Gaigneaux, P.E. Tsiakaras, D. Herla, L. Ghenne, P. Ruiz, B. Delmon, Catal. Today 33 (1997) 151.
[17] L.T. Weng, B. Delmon, Appl. Catal. A: Gen. 81 (1992) 141.
[18] L. Moens, P. Ruiz, B. Delmon, M. Devillers, Appl. Catal. A: Gen. 171 (1998) 131.
[19] L. Moens, P. Ruiz, B. Delmon, M. Devillers, Appl. Catal. A: Gen. 180 (1999) 299.
[20] F. De Smet, P. Ruiz, B. Delmon, M. Devillers, J. Phys. Chem. B 105 (2001) 12355.
[21] R.T. Sanderson, Science 114 (1951) 670.
[22] J.P. Jolivet, De la solution à l'oxyde, InterEditions/CNRS, 1994, p. 219.
[23] D.J. Buttrey, D.A. Jefferson, J.M. Thomas, Phil. Mag. A 53 (1986) 897.
[24] G.W. Keulks, L.D. Krenzke, T.M. Notermann, Adv. Catal. 27 (1978) 183.
[25] M.A. Subramanian, G. Aravamudan, G.V. Subba Rao, Prog. Solid State Chem. 15 (1983) 55.
[26] G.S.V. Coles, S.E. Bond, G. Williams, J. Mater. Chem. 4 (1994) 23.
[27] R.D. Shannon, J.D. Bierlein, J.L. Gillson, G.A. Jones, A.W. Sleight, J. Phys. Chem. Solids 41 (1980) 117.
[28] G. Malmros, Acta Chem. Scand. 24 (1970) 384.
[29] B. Delmon, P. Ruiz, S.R.G. Carrazan, S. Korili, M.A. Vicente Rodriguez, Z. Sobalik, Stud. Surf. Sci. Catal. 100 (1996) 1.